BIOCHEMISTRY
including biophysical chemistry & molecular biology

Article

pubs.acs.org/biochemistry

Tyrosine/Cysteine Cluster Sensitizing Human γD-Crystallin to Ultraviolet Radiation-Induced Photoaggregation in Vitro

Nathaniel Schafheimer,[†] Zhen Wang,[‡] Kevin Schey,[‡] and Jonathan King*[,†]

[†]Department of Biology, Massachusetts Institute of Technology, 68-330, 77 Massachusetts Avenue, Cambridge, Massachusetts 02139, United States

[‡]Department of Biochemistry, Vanderbilt University School of Medicine, Mass Spectrometry Research Center Suite 9160, MRB III, Nashville, Tennessee 37232, United States

Supporting Information

ABSTRACT: Ultraviolet radiation (UVR) exposure is a major risk factor for age-related cataract, a protein-aggregation disease of the human lens often involving the major proteins of the lens, the crystallins. γD-Crystallin (HγD-Crys) is abundant in the nucleus of the human lens, and its folding and aggregation have been extensively studied. Previous work showed that HγD-Crys photoaggregates in vitro upon exposure to UVA/UVB light and that its conserved tryptophans are not required for aggregation. Surprisingly, the tryptophan residues play a photoprotective role because of a distinctive energy-transfer mechanism. HγD-Crys also contains 14 tyrosine residues, 12 of which are organized as six pairs. We investigated the role of the tyrosines of HγD-Crys by replacing pairs with alanines and monitoring photoaggregation using light scattering and SDS-PAGE. Mutating both tyrosines in the Y16/Y28 pair to alanine slowed the formation of light-scattering aggregates. Further mutant studies implicated Y16 as important for photoaggregation. Mass spectrometry revealed that C18, in contact with Y16, is heavily oxidized during UVR exposure. Analysis of multiple mutant proteins by mass spectrometry suggested that Y16 and C18 likely participate in the same photochemical process. The data suggest an initial photoaggregation pathway for HγD-Crys in which excited-state Y16 interacts with C18, initiating radical polymerization.

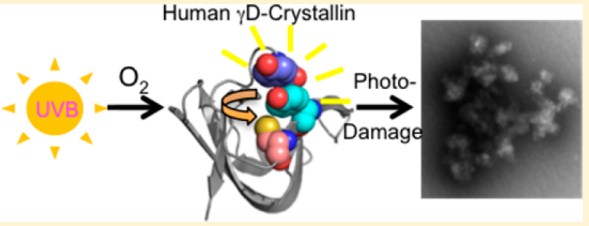

The eye lens is a unique tissue in the human body, responsible for maintaining transparency to allow the passage of light as well as producing refractive power to focus an image onto the retina. During lens formation, epithelial cells terminally differentiate into elongated fiber cells, wrapping onto an organized core of existing fiber cells. Thus, much of the body of the human lens is formed early in life.[1] In the process of differentiation, the cells produce large quantities of crystallin proteins, which become the major proteins of the lens fibers. As they mature and terminally differentiate, the fiber cells undergo enucleation, degrading their nuclei and other organelles and shutting down many metabolic functions.[2,3] Fully differentiated lens fiber cells do not produce or degrade proteins, so existing proteins must remain stable in solution for the lifetime of the individual.

Cataract is the leading cause of blindness in the world, projected to affect 30 million people in the United States alone by 2020.[4] Several variations of the disease exist, but the most prevalent is age-related cataract, affecting primarily the elderly. In the aging lens, damaged or misfolded proteins aggregate into insoluble high-molecular-weight complexes, scattering visible light and causing the lens to become opaque, blocking vision.[5−7] Currently, the only therapy is surgical removal of the cataractous lens and replacement with an artificial lens. Although this is effective and safe, it is costly and requires modern medical facilities. As populations age in many developed countries, cataract will become an increasing social and economic burden.[8]

Characterizations of lens proteins by mass spectrometry and immunohistochemistry have shown that over time covalent modifications, including deamidation, racemization, glycosylation, and oxidation, accumulate on lens proteins.[9−12] Several modifications that reduce protein stability and promote aggregation are more abundant in cataractous lenses than healthy lenses.[10,13,14] Although a number of factors are known to increase covalent modification and the risk of cataract, one ubiquitous hazard is solar ultraviolet radiation.

Ultraviolet radiation (UVR) in the UVA (320−400 nm) and UVB (280−320 nm) ranges can cause direct damage to living tissue through photochemical reactions with amino acids, nucleotides, and lipids[15−18] as well as indirect damage through the generation of reactive oxygen species (ROS) and subsequent oxidative damage. UVR exposure is associated in many tissues with increased mutation rates and cell death.[19,20] The lens is shielded from UVR beneath 295 nm by the cornea, but the long-lived nature of lens proteins means even relatively rare events can be significant to the pathology of cataract. Because of the lens' chronic exposure to light and lack of

Received: October 12, 2013
Revised: December 31, 2013
Published: January 13, 2014

protein turnover, photo-oxidative damage to lens proteins can accumulate over a lifetime.[15,21]

The crystallin family of proteins are the primary proteins of the human lens. Together, the α, β, and γ-crystallins make up more than 90% of total lens protein and are key to maintaining the translucency of the lens tissue for vision.[22] The β/γ-crystallins consist of two homologous domains; the β-crystallins are multimeric and contain N-terminal extensions, whereas the γ-crystallins are monomeric.[22−24] Both β- and γ-crystallins are highly stable, resisting denaturation by heat and chemicals.[25,26] The domain structure of each β/γ-crystallin consists primarily of β-sheet in the form of a double Greek Key fold in which the third strand of each key is exchanged with the other key. α-Crystallin, the major lens chaperone, is a member of the small heat shock protein family (sHSP) and consists of two subunits, αA-crystallin and αB-crystallin (HαB-Crys), which assemble into high-molecular-weight multimeric complexes.[27,28]

During refolding from the fully denatured state, the γD-crystallin chains populate a partially folded intermediate, with the N-terminal domain disordered and the C-terminal domain nativelike. The C-terminal face of the domain interface serves as a template for N-terminal folding.[29] At high protein concentrations, these partially folded species aggregate into high-molecular-weight light-scattering species.[25] In contrast, the native state, when incubated at low pH, forms well-formed amyloid fibers.[30,31] Using two-dimensional IR spectrosocpy and segmental ^{13}C labeling, Moran et al. identified domain-specific interactions present in the amyloid form.[32]

The β/γ-crystallins contain a number of highly conserved aromatic residues. An extensive literature exists documenting the importance of aromatic residues to protein stability and folding.[33−35] Clustering of aromatic and other hydrophobic amino acids drives the folding of polypeptide chains, and aromatics are key components of the water-tight hydrophobic core of the crystallins.[36] However, these residues also absorb light in the UV range, entering into short-lived singlet excited states from which they can fluoresce or undergo intersystem crossing, converting to longer-lived triplet excited states. These can participate in radical chemistry, leading to covalent damage and protein cross-linking.[15] In both excited states, tryptophan, tyrosine, and phenylalanine have been shown to transfer excited-state energy nonradiatively to other aromatics in close proximity (5−10 Å),[37,38] and in the triplet state, to molecular oxygen, generating singlet oxygen.[15,16] Singlet oxygen, like other reactive oxygen species (ROS), can react and cause oxidative damage to many biological targets, including the amino acids tryptophan, tyrosine, lysine, histidine, and cysteine.[15]

Previous work has investigated the effect of UVR on extracted lenses and lens proteins as well as ROS generated using photosensitizers. Bovine crystallin solutions exposed to photodynamically generated ROS became cloudy, and exposed proteins partitioned to the insoluble fraction.[39] Human and bovine crystallin solutions exposed to UVR also displayed a rise in turbidity, non-Trp fluorescence, protein oxidation, and protein cross-linking.[40−42] UVR has been found to cause cataract in a number of animal models, including guinea pig, squirrel, rat, and rabbit.[43−46]

Human γD-Crystallin (HγD-Crys) is a 173 amino acid protein, one of the more abundant γ-crystallins in the nucleus of the human lens, and a model for protein aggregation. Previous work has found that HγD-Crys aggregates when subjected to thermal denaturation and also when refolding from a guanidine-HCl fully denatured state.[47,48] At pH 3 or lower, HγD-Crys forms amyloid fibrils.[30]

HγD-Crys contains 4 tryptophans, 14 tyrosines, and 6 phenylalanines. The tryptophan residues are highly conserved across vertebrate β/γ-crystallins and arranged in homologous pairs. Previous work on HγD-Crys has explored the contributions of its high number of aromatic residues to folding and long-term stability.[49−51] Recent work by Chen et al. characterized an energy-transfer mechanism between tryptophan residues within a pair that rapidly dissipated excited-state energy down the protein backbone.[52,53] This was hypothesized to play a photoprotective role given the lens' chronic exposure to light. In silico work by Xia et al. simulated the effect of photodamage to the tryptophans, replacing the buried tryptophan with kynurenine, its photodamaged product.[36] Kynurenine replacement loosened the hydrophobic core of HγD-Crys, destabilizing the protein and speeding unfolding.

Previous experiments showed that HγD-Crys photoaggregates when exposed to UVR in vitro.[54] Recent work by Moran et al. found that HγD-Crys photoaggregated into amyloid-like structures when exposed to UVB,[55] primarily through interactions among strands of the C-terminus. The aggregated, high-molecular-weight states generated upon UV irradiation appear to include both amyloid and nonamyloid polymers.[54,55] Moran et al. concluded that the aggregation pathway involved loss of the native Greek Key fold and its reorganization.[55]

We have tried to identify the UVR-induced modification(s) that initiate and/or promote aggregation. By examining the photoaggregation of W:F mutants of HγD-Crys, we showed that the tryptophan energy-transfer mechanism played a protective role and also suggested that tryptophan was not a site of photodamage or cross-linking when HγD-Crys photoaggregated in vitro.[54]

If the tryptophan pairs act photoprotectively and are not major sites of photodamage, then some set of the remaining aromatic residues must participate as UVR absorbers and/or photodamage sites. Six pairs of interacting tyrosines and phenylalanines also exist across HγD-Crys (Figure 1). Four of these, Y6/F11, Y45/Y50, Y92/Y97, and Y133/Y138, are Greek Key pairs conserved between two HγD-Crys domains in homologous positions at β-hairpins.[51] Two pairs, Y16/Y28 and

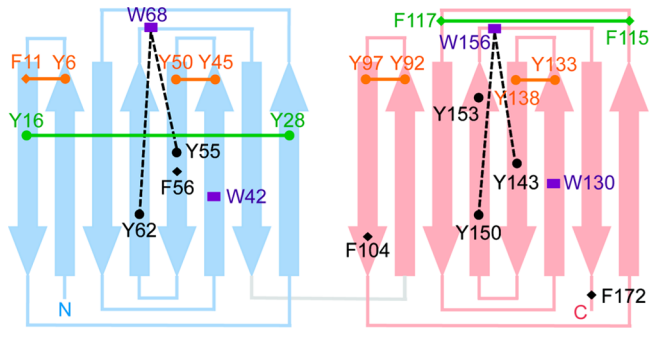

Figure 1. Schematic of aromatic residues in HγD-Crys, with the N-terminal domain in blue and the C-terminal domain in red. The positions of the aromatic amino acids are labeled with circles representing tyrosines, diamonds phenylalanines, and purple rectangles tryptophans. Connected orange residues are members of the Greek Key aromatic pairs, connected green residues are members of the non-Greek Key aromatic pairs, and black residues are not members of pairs, with dotted black lines showing participation in a tyrosine, tryptophan, tyrosine cluster.

F115/F117, are non-Greek Key pairs positioned at non-homologous locations. In addition, individual tyrosines Y62 and Y150 are also important as the Greek Key signature tyrosine corners, making structurally key hydrogen bonds with the peptide backbone of the next β-strand.[34] The tyrosine corners also form three-residue clusters with W68 and Y55 in the N-terminal domain and W156 and Y143 in the C-terminal domain. Recent work has examined the structural and folding roles of the tyrosine and phenylalanine pairs, showing that mutation of pairs to alanine significantly disturbs folding and stability for a given HγD-Crys domain.[51] In silico molecular dynamics experiments by Yang et al. have also shown that Y:A mutation of the tyrosine pairs destabilizes HγD-Crys, opening the hydrophobic cores to water.[56]

In this work, we investigated whether the aromatic pairs of HγD-Crys play a role in UVR-induced aggregation in vitro and the types of photodamage that occur during UVR exposure. We used double alanine mutant HγD-Crys constructs targeting the aromatic pairs and examined their photoaggregation behavior using light scattering to monitor the development of larger, late-stage aggregates and SDS-PAGE to monitor initial dimeric/multimeric photoproducts. We also used liquid chromatography coupled with electrospray ionization tandem mass spectrometry to search directly for photodamaged sites and to examine the photoaggregation behavior of cysteine-to-serine mutant constructs. In addition, C18 oxidation was quantitatively monitored with increasing irradiation time by multiple reaction monitoring (MRM) mass spectrometry. Using this data, we propose a mechanism for photoaggregation of HγD-Crys.

EXPERIMENTAL PROCEDURES

Mutagenesis, Expression, and Purification of HγD-Crys. N-terminally 6×-His tagged wild-type (WT) HγD-Crys expression constructs were modified via site-directed mutagenesis to introduce Y:A, F:A, and C:S substitutions as described previously.[49,51] All constructs were confirmed via sequencing (Genewiz).

Recombinant WT HγD-Crys and mutant proteins were expressed and purified as described previously[49] with several modifications. Cells were grown to OD_{600} ~1 in Super broth media at 37 °C with shaking. IPTG was added to 1 mM, and cultures were transferred to 18 °C followed by shaking overnight. Cells were pelleted by centrifugation for 20 min at 17 000*g* and resuspended in 30 mL of Ni-NTA lysis buffer (300 mM NaCl, 50 mM $NaPO_4$, and 18 mM imidazole, pH 8) containing two tablets of Roche complete EDTA-free protease inhibitor. After addition of lysozyme to 3 mg/mL and DNase to 3 μg/mL of lysate, pellets were lysed via ultrasonication and centrifuged at 17 000*g* for 45 min. Supernatants were filtered and applied to a Ni-NTA column (GE Healthcare). Protein was eluted using a linear gradient of increasing imidazole concentration. Fractions containing the protein of interest were pooled and dialyzed three times against storage buffer (10 mM ammonium acetate, pH 7.0). HγD-Crys was concentrated using 10 000 MWCO Vivaspin 20 concentrators (Sartorius Stedim Biotech).

Protein Concentration Measurement. Stock protein sample concentration was determined using absorbance at 280 nm with the following extinction coefficients (determined using SIB's ProtParam): WT, single C:S, NoCys, and double F:A HγD-Crys, 42 860 M^{-1} cm^{-1}; double Y:A HγD-Crys, 39 880 M^{-1} cm^{-1}; single Y:A HγD-Crys, 41 370 M^{-1} cm^{-1}; and quadruple W:F HγD-Crys, 20 860 M^{-1} cm^{-1}.

Photoaggregation Experiments. Samples of HγD-Crys were prepared at 1 mg/mL in 1× reaction buffer (100 mM Na_2PO_4 and 1 mM EDTA, pH 7). Samples were irradiated at room temperature in a quartz cuvette (Starna Group) using a UVP Inc. UVLMS-38 lamp equipped with a 302 nm midrange bulb delivering a range of UVA/UVB light. UVR dose delivery was set to 2 mW/cm^2 by adjusting the cuvette's distance to the lamp and was determined before each experiment by a UVX radiometer with midrange UVX-31 sensor. Turbidity readings at OD_{600} on a Cary UV/vis spectrometer were taken at regular time points during irradiation. Samples removed and analyzed via SDS-PAGE were reduced and boiled and electrophoresed through 14% acrylamide gels at 170 V for 1 h; gels were stained using Krypton fluorescent protein stain (Thermo Fisher Scientific) and imaged on a Typhoon 9400 (Amersham Biosciences). Gel band quantification was performed using ImageJ.

Mass Spectrometry Measurements. HγD-Crys samples for LC−MS/MS were prepared and irradiated as described in the photoaggregation section. Exposed samples (0 and 60 min) were mixed with SDS loading buffer lacking BME (to final concentration 333 mM Tris, pH 6.8, 2% SDS, and 30% glycerol). DTT was added to 10 mM, and samples were incubated for 1 h at 37 °C. Iodoacetamide was added to 55 mM, and samples were incubated for an additional hour in the dark at 37 °C.

Samples then underwent SDS-PAGE through a 14% acrylamide gel at 170 V for 1 h. The monomer and dimer gel bands were excised and destained with three consecutive washes of 50 mM ammonium bicarbonate/acetonitrile (ACN) (1:1, v/v) for 10 min each. The gel bands were then washed three times with 50 mM ammonium bicarbonate/ACN (1:1, v/v) for 10 min each. The dehydrated gel bands were completely dried by SpeedVac. Each sample containing an individual band was rehydrated in 10−15 μL of solution containing 10 ng/μL of trypsin or chymotrypsin (Promega) in 50 mM ammonium bicarbonate for 15 min. Fifty microliters of 50 mM ammonium bicarbonate buffer was added to each sample, and the samples were incubated at 37 °C for 18 h. Peptides were extracted using 20% ACN/0.1% formic acid (FA) once, 60% ACN/0.1% FA twice, and 80% ACN/0.1% FA once. The extract solutions were pooled and dried in by SpeedVac and reconstituted in 0.1% formic acid for subsequent LC−MS/MS analysis.

Peptides were separated on a one-dimensional fused silica capillary column (150 mm × 100 μm) packed with Phenomenex Jupiter resin (3 μm mean particle size, 300 Å pore size) using the following gradient at a flow rate of 0.5 μL/min: 0−10 min: 2% ACN (0.1% formic acid), 10−50 min: 2−35% ACN (0.1% formic acid), 50−60 min: 35−90% ACN (0.1% formic acid) balanced with 0.1% formic acid. The eluate was directly infused into a Velos Pro mass spectrometer or a Velos Orbitrap mass spectrometer (ThermoScientific) equipped with a nanoelectrospray source. Dynamic exclusion (repeat count, 2; exclusion list size, 300; and exclusion duration, 60 s) was enabled to allow detection of less-abundant ions for all LC−MS/MS analyses.

HγD-Crys samples for multiple reaction monitoring (MRM) mass spectrometry were prepared at 2 mg/mL in 1× reaction buffer and exposed to 2 mW/cm^2 UVR as in the photoaggregation experiments. Two-hundred microliter samples were removed at 0, 10, 20, 30, 40, 50, and 60 min of UVR exposure.

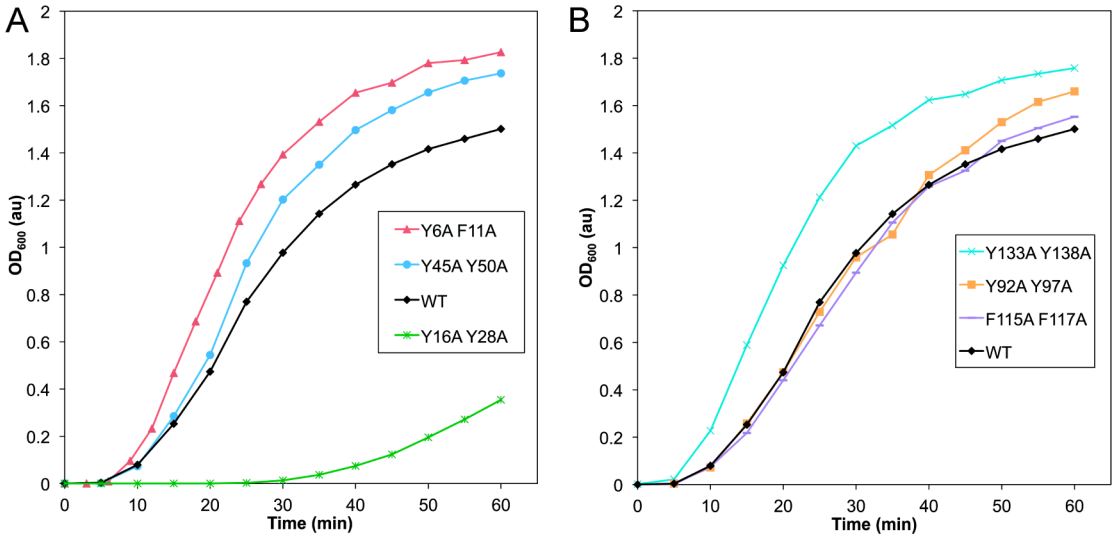

Figure 2. Comparison of UVR-induced aggregation of HγD-Crys constructs with aromatic pairs replaced by alanines. Samples were prepared at 1 mg/mL in reaction buffer, and light scattering was monitored at 600 nm during the UVR exposure time. (a) N-terminal pairs: WT (black diamonds), Y6A/F11A (red triangles), Y16A/Y28A (green hashes), and Y45A/Y50A (blue circles). (b) C-terminal pairs: WT (black diamonds), Y92A/Y97A (orange squares), F115A/F117A (lavender dashes), Y133A/Y138A (turquoise X's).

Time samples were centrifuged at 4 °C for 30 min at 17 000*g*, and the supernatant was removed and diluted 10-fold into guanidine HCl (GuHCl) buffer (final concentrations 5.5 M GuHCl, 100 mM sodium phosphate, pH 7, and 1 mM EDTA); these were labeled as the soluble fraction. The pellets were resuspended in 100 μL of GuHCl buffer and labeled as the pellet fraction. Soluble and pellet fraction time samples were incubated overnight at 37 °C followed by sequential addition of DTT to 10 mM and 1 h incubation at 37 °C and iodoacetamide to 55 mM and 1 h incubation at 37 °C in the dark. Soluble and pellet samples were then precipitated using a methanol/chloroform protocol to separate protein from GuHCl. After pellets were separated from supernatants, sample pellets were dried, rehydrated, and suspended in 30 μL of 2 M urea and 100 mM Tris HCl (pH 8.5). Porcine trypsin (Promega) was added to all samples to a final concentration of 16.7 ng/μL, and samples were incubated overnight at 37 °C. Digestions were stopped by adding 1.5 μL of 1% trifluoroacetic acid to each sample.

Samples were analyzed by multiple reaction monitoring (MRM) on a TSQ Vantage mass spectrometer (ThermoScientific). After an unscheduled run to determine retention times for peptides of interest, a scheduled MRM method was created using Skyline to include a 10 min window around the measured peptide retention time along with calculated optimum collision energies.[57] Q1 peak width resolution was set to 0.7, collision gas pressure was 1 mTorr, and an EZmethod cycle time of 5 s was utilized. The resulting RAW instrument files were imported into Skyline for peak-picking and quantitation. For relative quantitation of C18 trioxidation, the peak area for trioxidized peptide 15-31 was compared to the summed intensity of two peptides determined to be unchanged by UV irradiation: peptides 3-9 and 169-173.

Circular Dichroism Thermal Unfolding Measurements. CD spectra of the WT and mutant proteins were obtained using an AVIV model 202 CD spectrometer (Lakewood, NJ). Protein samples were prepared at a concentration of 0.1 mg/mL in 10 mM sodium phosphate, pH 7.0. Data were collected at 218 nm in a 1 cm quartz cuvette. Sample temperature was increased from 25 to 95 °C in 1 °C steps with 1 min of equilibration time per degree Celsius followed by 5 s reads. Data were corrected for buffer blank readings, and mean residue ellipticity was calculated. The mean residue ellipticity versus temperature data were fit to a sigmoidal curve using Kaleidagraph (Synergy Software), and the unfolding midpoints were calculated. The unfolding temperatures reported are averages of three thermal unfolding experiments.

RESULTS

Photoaggregation of Aromatic Pair Mutants. To investigate the potential roles of the aromatic pairs in the photoaggregation of HγD-Crys, we employed HγD-Crys double mutant proteins in which both members of an aromatic pair were mutated to alanine. We exposed these mutant HγD-Crys proteins to 2 mW/cm^2 UVR for 60 min while monitoring aggregation using light scattering at 600 nm (Figure 2a,b). Two of the three N-terminal mutant pairs, Y6A/F11A and Y45A/Y50A, and one of the C-terminal mutant pairs, Y133A/Y138A, photoaggregated slightly more quickly than WT, indicating their loss likely made HγD-Crys slightly more vulnerable to UVR. Two of the C-terminal mutants, Y92A/Y97A and F115A/F117A, behaved similarly to WT, indicating they had no effect on HγD-Crys photoaggregation. One N-terminal pair mutant, Y16A/Y28A, photoaggregated significantly slower than WT, suggesting that one or both residues are important participants in photodamage.

The differences in photoaggregation between the aromatic pair mutants suggested that specific tyrosines and phenylalanines of HγD-Crys are distinct in their absorptive and photochemical properties. Because absorbed energy can be transferred between nearby aromatic amino acids, the pair mutants that photoaggregated more quickly and severely than WT could have roles transferring energy to the highly conserved tryptophan pairs previously shown to play a protective role.[52,58] Light scattering eventually developed at longer UVR exposure times in the Y16A/Y28A samples,

suggesting that other photodamage sites must still be operating in the absence of these tyrosines.

Photoaggregation of C:S Mutant HγD-Crys. To identify the sites that are modified after UVR treatment, irradiated HγD-Crys protein was digested by protease treatment, and the resulting peptides were analyzed by mass spectrometry. C18, and to a much lesser extent C78 and C108, were identified as sites of oxidative damage after UVR exposure (Supporting Information Figure 1). Cysteine thiols were oxidized to sulfinic and sulfonic acid.

To determine the importance of the individual cysteine residues identified via mass spectrometry in photoaggregation, we constructed HγD-Crys mutant constructs with cysteines of interest mutated to serines. We exposed the purified proteins to UVR, monitoring turbidity as with the aromatic pair mutants (Figure 3). C78S HγD-Crys and C108S HγD-Crys both behaved similarly to WT or aggregated slightly more rapidly, suggesting their oxidation might have been unrelated to aggregation.

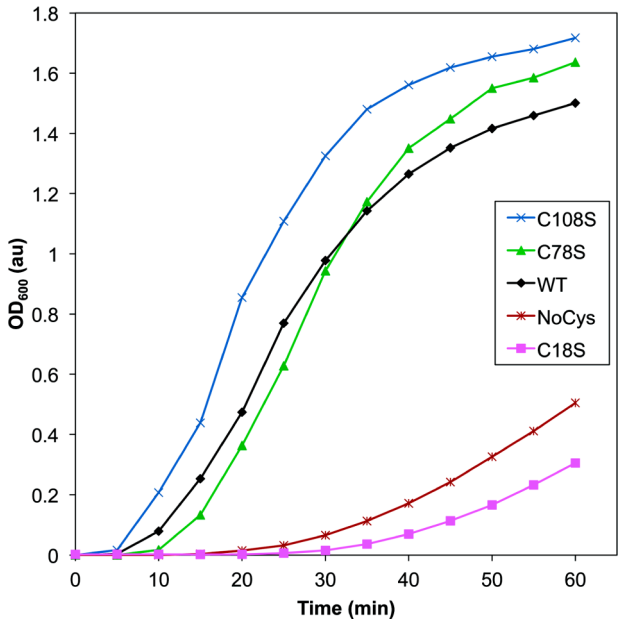

Figure 3. Comparison of UVR-induced aggregation of HγD-Crys constructs with select cysteine residues replaced with serines. Samples contained protein at 1 mg/mL in reaction buffer, and light scattering was monitored at 600 nm as a function of UVR exposure time: WT (black diamonds), C18S (magenta squares), C78S (green triangles), C108S (blue X's), and NoCys (maroon hashes).

C18S HγD-Crys photoaggregated much more slowly than WT, suggesting that C18 played an important role in HγD-Crys photoaggregation. This is consistent with the mass spectrometry data, which showed a much higher abundance of C18 oxidation than C78 or C108 in both soluble and aggregated pellet fractions, suggesting it more readily reacts with ROS (Supporting Information Figure 2). In addition, mass spectrometry data showed that C18 oxidation in the aggregated pellets was present at higher levels than in the soluble fraction, supporting a role for C18 oxidation during protein aggregation (Supporting Information Figure 3). It seems unlikely that the oxidation product of C18 by itself produces a covalent photocross-link, but it could be involved in the formation of noncovalent protein interactions contributing to aggregation.

Prior experiments using SDS-PAGE revealed a dimerlike gel band that appeared immediately upon UVR exposure of HγD-Crys and suggested the formation of covalent photoproducts preceding or separate from the development of light-scattering aggregates.[54] The complete oxygen dependence of in vitro photoaggregation established that ROS were required during UVR exposure and also suggested that aggregates possessed at least a partially covalent character.[54] In light of this data, HγD-Crys photoaggregates may form through free-radical polymerization, for example, through a transient thiol radical. The stable C18 oxidation product may be an off-pathway photodamage reaction in competition with a C18-related aggregation pathway.

Cysteine thiol groups have been shown to participate in radical photochemistry that produces cross-links to a variety of chemical groups.[59−61] Fu et al. observed intra- and intermolecular cross-linking mediated by cysteine thiols when synthetic peptides were exposed to hypochlorous acid.[62] Given the oxidation of C18, it seems likely that a cysteine radical could also be produced. Thiol radicals might be expected to form thio−ether cross-links to many residues on the surface of HγD-Crys. Intramolecular cross-links would require a high degree of resolution to identify, and the heterogeneity of these cross-links would make them difficult to discover by mass spectrometry.

To determine the extent of photoaggregation of HγD-Crys in the absence of cysteine, we created a multiple mutant HγD-Crys construct, NoCys, with all six cysteines mutated to serine. When exposed to UVR, the NoCys HγD-Crys protein photoaggregated, but the rate of photoaggregation was slowed as compared to WT and was similar to C18S HγD-Crys (Figure 3). This suggested that C18 may be the only HγD-Crys cysteine important for photoaggregation, as removing all cysteines retarded photoaggregation to a similar extent as mutating C18.

The NoCys HγD-Crys protein still exhibited some delayed photoaggregation, so other sites may be involved in secondary-photoaggregation pathways. NoCys HγD-Crys was extremely destabilized relative to WT HγD-Crys (Table 1), but it still photoaggregated much more slowly than WT, demonstrating that overall thermodynamic stability does not appear to play a significant role in photoaggregation propensity.

Table 1. Circular Dichroism Thermal Unfolding Data for HγD-Crys Mutant Constructs

construct	melting temperature (°C)	standard deviation (°C)
WT	82.1	0.4
Y16A	77.3	0.07
Y28A	76.9	0.04
C18S	72.5	0.3
Y16A Y28A	75.3	0.07
Y16A C18S	73.2	0.13
C18S Y28A	73.3	0.1
Y16A C18S Y28A	72.3	0.06
NoCys	59.6	0.08

Analyzing Mutants of the Y16/C18/Y28 Cluster. In the high-resolution HγD-Crys crystal structure by Slingsby and coworkers, the thiol group of C18 is in direct contact with the aromatic ring of Y16, which is itself stacked in a pair with Y28.[23] To investigate the relationships among these three residues implicated in photoaggregation, we made different individual

dx.doi.org/10.1021/bi401397g | Biochemistry 2014, 53, 979−990

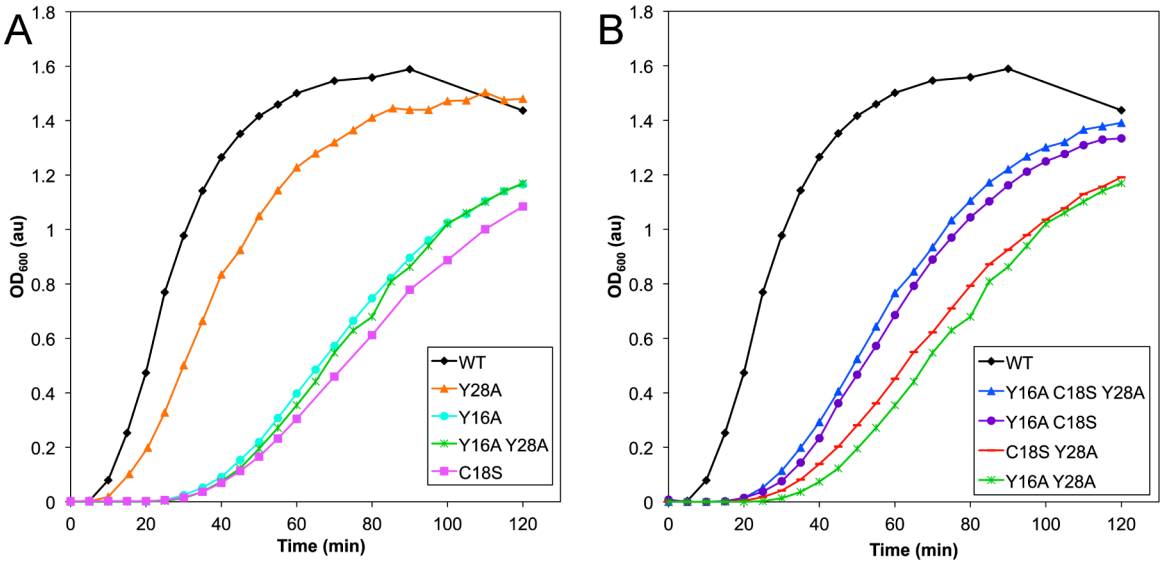

Figure 4. Comparison of UVR-induced aggregation of HγD-Crys constructs with individual or combination mutations of C18S, Y16A, and Y28A. Samples were prepared at 1 mg/mL in reaction buffer, and light scattering was monitored at 600 nm during UVR exposure time. (A) WT (black diamonds), Y16A (turquoise circles), C18S (magenta squares), Y28A (orange triangles), and Y16A/Y28A (green hashes). (B) WT (black diamonds), Y16A/Y28A (green hashes), Y16A/C18S (purple circles), C18S/Y28A (red dashes), and Y16A/C18S/Y28A (blue triangles).

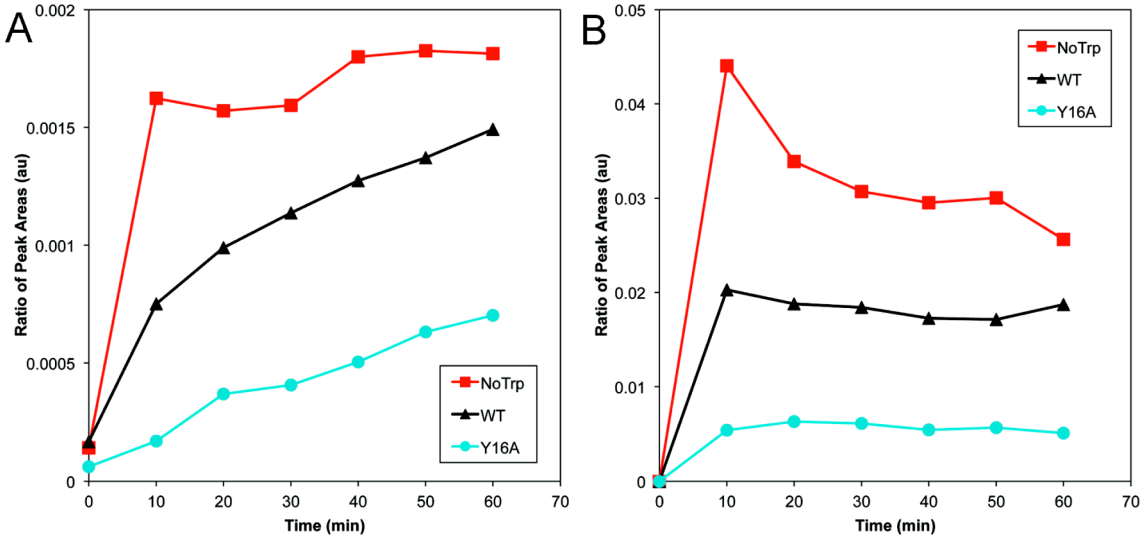

Figure 5. MRM mass spectrometry monitoring C18 trioxidation. Quantitation of trioxidized peptide 15-31 for UVR-exposed WT, Y16A, and NoTrp HγD-Crys as a function of exposure time. The *y* axis plots the 15-31 peptide peak area divided by peak areas for peptides 3-9 and 169-173 for internal protein loading control. (a) Soluble UVR-exposed protein samples and (b) pelleted photoaggregated protein samples, with WT (black triangles), Y16A (turqouise circles), and NoTrp (red squares).

and combination mutant HγD-Crys constructs of the three sites and compared the mutant protein photoaggregation behavior by monitoring turbidity (Figure 4a,b).

The Y16A HγD-Crys single mutant displayed retarded photoaggregation as compared to WT, similar to C18S and Y16A/Y28A HγD-Crys. Y28A HγD-Crys photoaggregation was only mildly delayed and much more similar to WT. This suggested that for photoaggregation Y16 is the important tyrosine of the Y16A/Y28A pair tested earlier (Figure 2). Because of the similarity in photoaggregation rates of Y16A and C18S HγD-Crys, it is likely that the slowing of photoaggregation in each single mutant was due to removal of a shared activity dependent on the presence of both residues. Therefore, we postulate that mutating one residue would be sufficient to abolish the relevant photochemical activity of both. Additionally, Y28A HγD-Crys' mild photoaggregation retardation as compared to WT may have nothing to do with its own participation in photochemistry and could simply be a consequence of Y28's proximity to Y16 and C18.

Y16A/C18S HγD-Crys, C18S/Y28A HγD-Crys, and triple mutant Y16A/C18S/Y28A HγD-Crys were exposed to UVR and compared to Y16A/Y28A HγD-Crys and WT to investigate the interplay between the three residues. C18S/Y28A HγD-Crys behaved similarly to C18S and Y16A/Y28A, suggesting again that Y28 is not important for photoaggregation and that the mutation of C18 or Y16 is sufficient to produce the observed retardation.

Curiously, the Y16A/C18S double mutant HγD-Crys and triple mutant Y16A/C18S/Y28A HγD-Crys photoaggregated at an intermediate rate between Y16A/Y28A and WT HγD-Crys.

dx.doi.org/10.1021/bi401397g | *Biochemistry* 2014, 53, 979−990

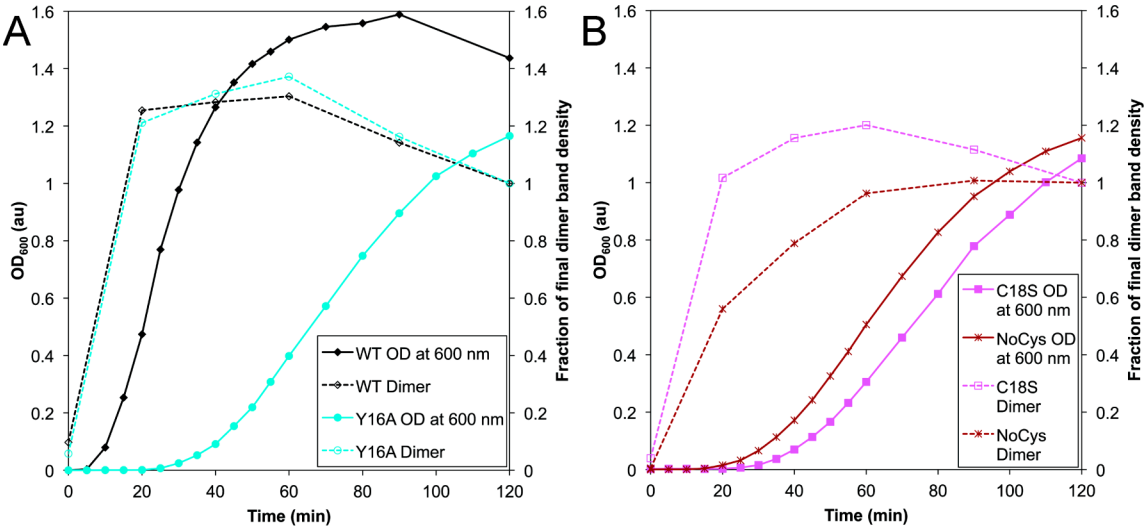

Figure 6. Comparing turbidity to dimeric product formation with Y16A, C18S, NoCys, and WT HγD-Crys. Comparison of turbidity development at 600 nm (left axis, solid lines and closed symbols) and density of dimer gel band (right axis, dotted lines and open symbols) versus UVR-exposure time for 4 HγD-Crys constructs. Samples were prepared at 1 mg/mL in reaction buffer. Twenty microliters of samples was added to 10 μL of 3× gel loading buffer, the samples were boiled, and then 15 μL was electrophoresed. Dimer band density was normalized to final dimer band density to give the fraction of final dimer band density. (a) WT (black diamonds) and Y16A (turquoise circles) and (b) C18S (magenta squares) and NoCys (maroon hashes).

The simple lack of an additive delay when Y16 and C18 were both mutated away is further evidence that they participate in a single photochemical process. However, the moderate increase in photoaggregation rate over the single mutants when the Y16A and C18S mutations are put together suggested that although the double mutation abolishes the photochemistry that Y16 and C18 are involved in it increases the rate of some other photoaggregation related reaction, perhaps by subtly perturbing the structure of the N-terminal domain. A similar analysis applies to the Y16A/C18S/Y28A triple mutant HγD-Crys, and its similarly intermediate behavior to Y16A/C18S HγD-Crys is further evidence of the peripheral photoaggregation activity of Y28.

MRM Mass Spectrometric Analysis of C18 Trioxidation. To test the hypothesis that Y16 and C18 are involved in the same photochemical-damage mechanism, targeted MRM mass spectrometric analysis was performed to compare levels of tryptic HγD-Crys peptide 15-31 in UVR-exposed WT and Y16A HγD-Crys (Figure 5). The abundance of the trioxidized, sulfonic acid form of tryptic HγD-Crys peptide 15-31 from soluble or pelleted photoaggregate samples was monitored as a function of UVR-exposure time. The amount of peptide containing C18 oxidized to sulfonic acid rose in a UVR dose-dependent manner for both WT and Y16A HγD-Crys soluble protein samples, whereas the pelleted samples were steadily much higher than the soluble samples. However, the amount of trioxidized peptide in the Y16A samples was much lower than in WT and rose more slowly in the soluble samples. This supports the idea that Y16 and C18 are a single photochemically linked site. Disrupting one residue disrupted both the photochemistry and photoaggregation effect of the site.

Previously, we determined that the four tryptophans of HγD-Crys played a protective role against photoaggregation.[54] It seemed likely that this protective role involved minimizing photochemical damage to the aromatic residues. It is also possible that the tryptophan energy-transfer mechanism could be protective against other types of photodamage. To test whether the tryptophans played a role in C18 oxidation, we examined UVR-exposed NoTrp HγD-Crys via the same MRM mass spectrometry experiment as WT and Y16A HγD-Crys (Figure 5). NoTrp HγD-Crys showed higher amounts of C18 oxidation to sulfonic acid, and oxidation appeared more rapidly than WT or Y16A, suggesting that the photoprotective effect of the tryptophans extends to C18 oxidation.

Early- versus Late-Stage Photoaggregation. Monitoring UVR-exposed HγD-Crys with SDS-PAGE revealed the development of initial cross-linked dimeric photoproducts.[54] This early dimerization was differentiated from the later rise in larger, visible light-scattering aggregates. We used the same comparison to determine whether the Y16A, C18S, and NoCys mutations affect early- or late-stage photoaggregation (Figure 6a,b). When WT HγD-Crys was exposed to UVR, dimers appeared quickly, before light scattering. Despite the significant delay in light-scatter development seen with the Y16A, C18S, and NoCys mutants, all three developed photodimers at early times, similar to WT. This indicated that the photochemical process(es) that involve C18 and Y16 influence the light scattering late-stage of photoaggregation but not the early stage dimer formation. The formation of dimeric photoproducts when NoCys HγD-Crys protein was exposed to UVR also conclusively demonstrated that the dimer-producing cross-link does not involve cysteine.

DISCUSSION

The initiation of UVR-induced protein damage proceeds from absorption of UV photons. The photoaggregation monitored in the above experiments depended on the presence of oxygen.[54] Aggregation rapidly slowed after turning off the UVR source, indicating that dark reactions were a very minor component of the aggregation reaction (Supporting Information Figure 4). Thus, photoaggregation appears to depend on excited states of UVR-absorbing components of HγD-Crys interacting with ROS. Although the four buried and conserved tryptophans are the most efficient absorbers of UV photons in HγD-Crys, these residues are not required for the major photoaggregation pathway. In fact their UVR absorption and subsequent

dx.doi.org/10.1021/bi401397g | Biochemistry 2014, 53, 979−990

quenching appears to be photoprotective.[54] Moran et al. reported photo-oxidation of Trp130 (and Histidine 121).[55] These changes were found after many hours of UVR exposure and were not coupled to the initiation of aggregation.

The next most efficient UVR absorbers are tyrosine residues. The results reported here show that one pair of tyrosines, N-terminal Y16/Y28, together with neighboring C18 appear to be important to the in vitro photoaggregation of HγD-Crys. What differentiates Y16 and Y28 from the other five tyrosine pairs whose replacement by alanine did not significantly affect photoaggregation?

Solvent exposure and the proximity of amino acid side chains known to undergo radical chemistry mark Y16 and Y28 as different from other aromatic pairs (Figure 7). In the HγD-Crys crystal structure, both Y16 and Y28 are surface-exposed compared to other aromatic pairs, making it more likely for them to encounter molecular oxygen and perhaps more prone to participate in an intermolecular cross-link. Additionally, the Y16/Y28 pair is the only pair in the HγD-Crys crystal structure with a cysteine thiol (C18) contacting an aromatic ring. There is also a histidine, H22, in close proximity to Y16 and Y28. Both the thiol and imidazole side chains have been shown to participate in radical photochemistry, for example, in the cysteine-based variants of thiol-ene click chemistry or in the formation of histidine−histidine or histidine−lysine cross-links via singlet oxygen.[60,63]

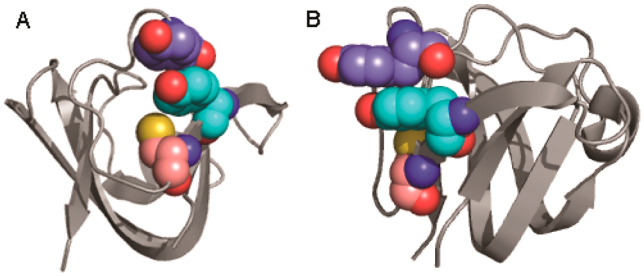

Figure 7. Three-dimensional structure of HγD-Crys N-terminal domain highlighting Y16, Y28, and C18. Ribbon structure of the N-terminal domain of HγD-Crys highlighting the identified key residues for photoaggregation as spheres: Y16 (turquoise carbons), Y28 (indigo carbons), and C18 (salmon carbons). Panels A and B are approximately 90° rotations of the same structure, highlighting the positioning of the three residues relative to each other.

Y16 and Y28 are members of the N-terminal non-Greek Key aromatic pair and are not as strongly conserved across βγ-crystallins as the Greek Key pairs.[51] Kong et al. aligned the sequences of 79 β/γ-crystallin protein sequences across eight species and found that Y16 and Y28 were only conserved across 44% of sequences, primarily in the γ-crystallins, whereas the Greek Key pairs were conserved across 82−100%. It is possible that selective pressures for structural stability and against photoaggregation propensity are at odds with respect to the Y16/Y28 aromatic pair. The C-terminal non-Greek Key aromatic pair mutant, F115A/F117A HγD-Crys, although also poorly conserved, photoaggregated similarly to WT, suggesting no similarity to its N-terminal counterpart in this regard. This homologous C-terminal pair also lacks a neighboring cysteine.

The oxygen dependence of the in vitro photoaggregation of HγD-Crys[54] strongly favors a mechanism of indirect photodamage with singlet oxygen mediating cross-linking and photooxidation.[15,16] The major modified side chains detected by mass spectrometry were C18, C78, and C108. ROS-mediated cross-links and oxidation can target a number of amino acids, and as such, there could be additional minor sites of photodamage too low in abundance to be detected by our methods.[15]

Because the aggregated protein was not solubilized by boiling in SDS in the presence of reducing agents, it seemed likely that the protein molecules were covalently cross-linked. However, we did not recover cross-linked peptides. If aggregation proceeds by free-radical polymerization, for example, through

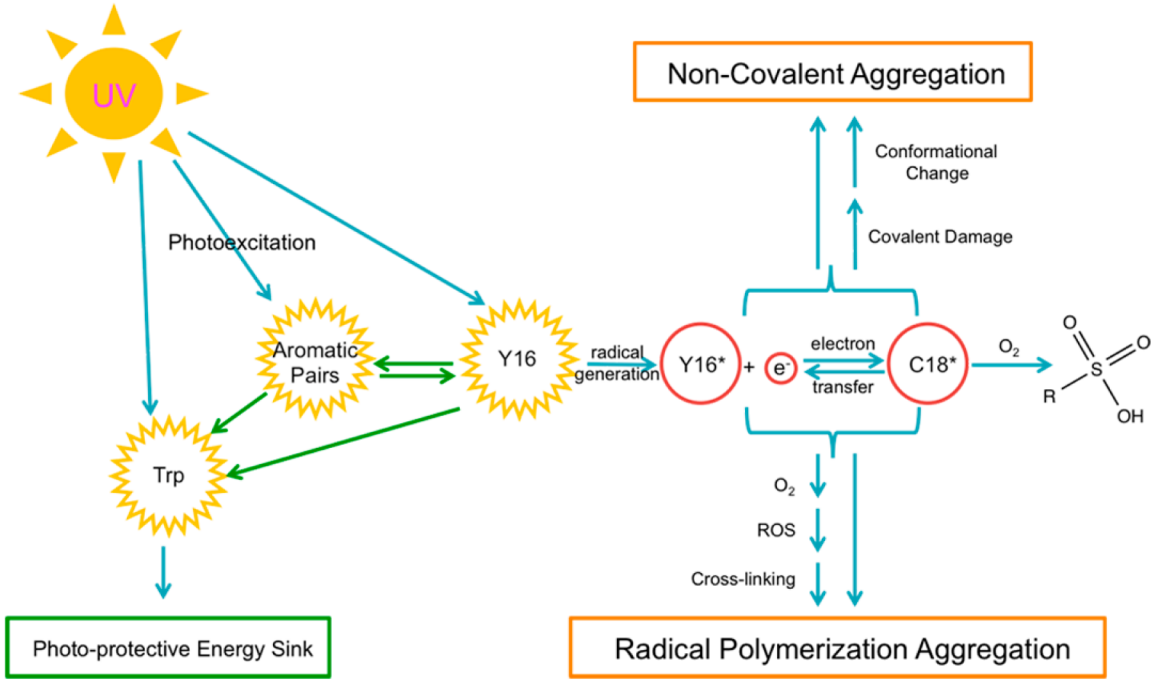

Figure 8. Model for in vitro photoaggregation of HγD-Crys.

dx.doi.org/10.1021/bi401397g | *Biochemistry* 2014, 53, 979−990

tyrosyl or cysteine radicals, then the cross-links could be very diverse so that no single cross-linked peptide species was well-populated.

The covalent changes in irradiated crystallin described here occurred at the beginning of the aggregation reaction, as monitored by turbidity and SDS-PAGE. The side-chain oxidation and fragmentation reported by Moran et al. were associated with later changes in the irradiated proteins.[55] Moran et al. showed by FTIR that their aggregated material contained amyloid structure.[32,55,64] Well-formed amyloid fibrils have been reported and described upon incubation of γ-crystallins at pH 3.[30,31] Previous experiments examining the UVR-induced aggregates of WT HγD-Crys using transmission electron microscopy revealed their morphology to be lumpy and irregular, distinctly non-amyloid-like.[54] However, our aggregated state could have included amyloid species. This material requires further characterization.

Photocross-linked species are likely resistant to protease digestion, as the native β/γ-crystallin family proteins have proven to be (data not shown); the denaturants present in our digestion reactions may be insufficient to produce a trypsin-digestible substrate. It is also possible that large cross-linked peptides are resistant to extraction from the gel. This would explain why we observe complete peptide coverage but primarily for unmodified peptides. This could also explain why mass spectrometric analysis of gel bands containing dimeric photoproducts did not identify cross-linked peptides. Moran et al. also did not recover cross-linked peptides under conditions in which they obtained 94% sequence coverage.[55] They did find semitryptic covalent fragments, with one terminus clustered around tryptophans 42 and 130.

From the current study of the aromatic pairs and the previously investigated protective role of the conserved tryptophan pairs,[54] we can envisage a photoaggregation mechanism involving radical polymerization and noncovalent association of HγD-Crys, as shown in Figure 8. Y16 can absorb a UV photon, entering into an excited state. It can transfer its excited-state energy nonradiatively to other aromatic residues, themselves excitable by UVR. Homotransfer of excited-state energy between aromatic amino acids is well-established,[37,38] and the high number of aromatic residues in HγD-Crys means no aromatic residue is more than ∼10 Å from another. These excited aromatic residues can transfer their energy to the conserved tryptophan pairs, which have been shown to transfer energy very efficiently from W42 to W68 and W130 to W156, respectively, dissipating it without undergoing photochemistry.[52,53,65] In this model, the tryptophan pairs act photoprotectively as a sink for excitation energy.

Y16 (or Y28), unlike the other aromatic residues examined, is on the surface of HγD-Crys and might transfer its excited state to molecular oxygen, generating singlet oxygen. Singlet oxygen can react at a number of sites on HγD-Crys. Y16 can also participate in radical chemistry while excited,[15,16] creating a tyrosyl radical and a free radical. C18's thiol group, in contact with Y16's aromatic ring, could react with Y16*, generating a thiol radical; if the exchange of the radical electron is reversible, then this might stabilize these intermediate photoproducts, increasing the likelihood of a damaging reaction or generation of ROS. Thiol and tyrosyl radicals can also interact with molecular oxygen, generating superoxide radical, which can, like singlet oxygen, target a number of sites on HγD-Crys, causing cross-linking and photoaggregation. The exposure-time-dependent build up of C18 oxidation products observed via mass spectrometry indicates a competing side reaction where ROS oxidize C18. The reduction in this side-reaction product, as observed via MRM mass spectrometry when Y16 is mutated to alanine, is strong evidence for photochemical interaction of C18 and Y16, and the significant increase in C18 trioxidation in the NoTrp mutant suggests a link between photodamage to C18 and the tryptophan photoprotective role.

Other photodamage sites besides the Y16/Y28 pair and C18 must exist, as photoaggregation occurred in their absence, but these were either too heterogeneous or too low in abundance to be detected.

The formation and molecular basis of the initial photodimer of HγD-Crys remains obscure. Because it presented as a distinct band after boiling, reduction, and SDS-PAGE, we can be reasonably sure that it is covalent and nondisulfide based. However, none of the sites studied via mutagenesis in this work appeared to be involved in the initial dimer's formation. It is likely that the initial dimer is an off-pathway photoproduct without relevance to light-scattering photoaggregation. However, the first step in a polymerization scheme is the linking of two individual monomers, and because initial dimer formation occurs before light-scattering development, the dimer is still plausibly the first intermediate on the path toward photoaggregation. Alternatively, the fast-forming, gel-visible dimers could be protective dead-ends in which ROS cause cross-linking that leads to less photoaggregation-prone species.

The lens is a very different environment from the test-tube conditions here. Besides maintaining a protein concentration of 200−400 mg/mL,[22] lens fiber cells have several defense mechanisms against photo-oxidative damage: free UV filter molecules consisting of kynurenine/tryptophan derivatives, the thioredoxin system, and the thioltransferase system.[66−68] Additionally, the lens, an avascular, bloodless tissue, maintains very low oxygen levels.[69] Despite this, the oxygen-dependent photocross-linking observed in this study in vitro is likely still very physiologically relevant to cataract. Protein damage leading to aggregation and cataract develops over the course of a human lifetime; on such a timeline, even relatively rare damage events such as those dependent on oxygen can be significant to pathological outcomes. Additionally, eye injury or surgery drastically raises the oxygen level of the lens, likely making photo-oxidative damage a greater threat to lens proteins.

As our understanding of protein photodamage in the lens increases, so too do our options for retarding cataract formation. Giblin, Andley, and colleagues have shown that UVR-blocking contact lenses prevent the UVR-induced opacification of lab-animal lenses.[45,70,71] Carnosine, an inhibitor of ROS-generating lipid peroxidation, shows promise as an anticataract drug.[72−74] HαB-Crys peptide fragments injected into animal cataract models have been shown to suppress aggregation and protein oxidation.[75] The identification of specific sites important to HγD-Crys photoaggregation will continue to inform these efforts.

The extensive literature on UVR damage to DNA has focused on the multiple enzymatic systems that cells have for repairing damaged DNA. It may be that some proteins play a role in protecting DNA from photodamage. The protein Absent in Melanoma (AIM1) appears to play some tumor-protective role in skin cells.[76] AIM1 has a sequence and conformation related to the lens γ- and β-crystallins and may be protecting skin cells by absorption and dispersion of UV photons. Thus, the photobiology of the lens crystallins may provide insights into other UVR-linked pathologies.

■ ASSOCIATED CONTENT

Supporting Information

Tandem mass spectrum of HγD-Crys peptide 15-31 with trioxidation on C18; selected ion chromatograms of HγD-Crys peptides 99-114 and 15-31 in trypsin digested UV-irradiated samples; and turbidity curves of WT HγD-Crys removing the UVR source at various times. This material is available free of charge via the Internet at http://pubs.acs.org.

■ AUTHOR INFORMATION

Corresponding Author

*E-mail: jaking@mit.edu. Phone: (617) 253-4700.

Funding

This work was supported by a grant from the National Eye Institute (EY015834).

Notes

The authors declare no competing financial interest.

■ ACKNOWLEDGMENTS

The Biophysical Instrumentation Facility for the Study of Complex Macromolecular Systems (NSF-007031) is gratefully acknowledged.

■ REFERENCES

(1) Augusteyn, R. C. (2008) Growth of the lens: In vitro observations. *Clin. Exp. Optom. 91*, 226−239.
(2) Bassnett, S. (2009) On the mechanism of organelle degradation in the vertebrate lens. *Exp. Eye Res. 88*, 133−139.
(3) Wride, M. A. (2011) Lens fibre cell differentiation and organelle loss: Many paths lead to clarity. *Philos. Trans. R. Soc., B 366*, 1219−1233.
(4) Congdon, N., Vingerling, J. R., Klein, B. E. K., West, S., Friedman, D. S., Kempen, J., O'Colmain, B., Wu, S.-Y., Taylor, H. R., and Group, E. D. P. R. (2004) Prevalence of cataract and pseudophakia/aphakia among adults in the United States. *Arch. Ophthalmol. 122*, 487−494.
(5) Friedrich, M. G., Lam, J., and Truscott, R. J. W. (2012) Degradation of an old human protein. Age-dependent cleavage of γS crystallin generates a peptide that binds to cell membranes. *J. Biol. Chem. 287*, 39012−39020.
(6) Kamei, A., Iwata, S., and Horwitz, J. (1987) Characterization of water-insoluble proteins in human lens nuclei. *Jpn. J. Ophthalmol. 31*, 433−439.
(7) Oyster, C. W. (1999) *The Human Eye: Structure and Function*, Sinauer Associates, Inc., Sunderland, MA.
(8) (2007) *The economic impact of vision problems*, pp 1−24, Report from Prevent Blindness America, Chicago, IL.
(9) Atalay, A., Ogus, A., Bateman, O., and Slingsby, C. (1998) Vitamin C induced oxidation of eye lens gamma crystallins. *Biochimie 80*, 283−288.
(10) Takata, T., Oxford, J. T., Demeler, B., and Lampi, K. J. (2008) Deamidation destabilizes and triggers aggregation of a lens protein, βA3-crystallin. *Protein Sci. 17*, 1565−1575.
(11) Fujii, N., Kawaguchi, T., Sasaki, H., and Fujii, N. (2011) Simultaneous stereoinversion and isomerization at the Asp-4 residue in βB2-crystallin from the aged human eye lenses. *Biochemistry 50*, 8628−8635.
(12) Ranjan, M., Nayak, S., Kosuri, T., and Rao, B. S. (2008) Immunochemical detection of glycated lens crystallins and their circulating autoantibodies in human serum during aging. *Mol. Vision 14*, 2056−2066.
(13) Flaugh, S., Mills, I., and King, J. (2006) Glutamine deamidation destabilizes human γD-crystallin and lowers the kinetic barrier to unfolding. *J. Biol. Chem. 281*, 30782.
(14) Beebe, D. C., Holekamp, N. M., and Shui, Y. B. (2010) Oxidative damage and the prevention of age-related cataracts. *Ophthalmic Res. 44*, 155−165.
(15) Davies, M. J., and Truscott, R. J. (2001) Photo-oxidation of proteins and its role in cataractogenesis. *J. Photochem. Photobiol., B 63*, 114−125.
(16) Pattison, D. I., Rahmanto, A. S., and Davies, M. J. (2011) Photo-oxidation of proteins. *Photochem. Photobiol. Sci. 11*, 38.
(17) Cadet, J., Mouret, S., Ravanat, J. L., and Douki, T. (2012) Photoinduced damage to cellular DNA: Direct and photosensitized reactions. *Photochem. Photobiol. 88*, 1048−1065.
(18) Williams, D. L. (2006) Oxidation, antioxidants and cataract formation: A literature review. *Vet. Ophthalmol. 9*, 292−298.
(19) Cao, C., and Wan, Y. (2009) Parameters of protection against ultraviolet radiation-induced skin cell damage. *J. Cell. Physiol. 220*, 277−284.
(20) Friedberg, E. C. (2001) How nucleotide excision repair protects against cancer. *Nat. Rev. Cancer 1*, 22−33.
(21) Dillon, J. (1994) UV-B as a pro-aging and pro-cataract factor. *Doc. Ophthalmol. 88*, 339−344.
(22) Bloemendal, H., de Jong, W., Jaenicke, R., Lubsen, N. H., Slingsby, C., and Tardieu, A. (2004) Ageing and vision: Structure, stability and function of lens crystallins. *Prog. Biophys. Mol. Biol. 86*, 407−485.
(23) Basak, A., Bateman, O., Slingsby, C., Pande, A., Asherie, N., Ogun, O., Benedek, G. B., and Pande, J. (2003) High-resolution X-ray crystal structures of human γD crystallin (1.25Å) and the R58H mutant (1.15Å) associated with aculeiform cataract. *J. Mol. Biol. 328*, 1137−1147.
(24) Bax, B., Lapatto, R., Nalini, V., Driessen, H., Lindley, P. F., Mahadevan, D., Blundell, T. L., and Slingsby, C. (1990) X-ray analysis of beta B2-crystallin and evolution of oligomeric lens proteins. *Nature 347*, 776−780.
(25) Fu, L., and Liang, J. J. (2002) Unfolding of human lens recombinant βB2- and γC-crystallins. *J. Struct. Biol. 139*, 191−198.
(26) Bateman, O. A., Sarra, R., van Genesen, S. T., Kappé, G., Lubsen, N. H., and Slingsby, C. (2003) The stability of human acidic β-crystallin oligomers and hetero-oligomers. *Exp. Eye Res. 77*, 409−422.
(27) Horwitz, J. (2003) Alpha-Crystallin. *Exp. Eye Res. 76*, 145−153.
(28) Laganowsky, A., Benesch, J. L. P., Landau, M., Ding, L., Sawaya, M. R., Cascio, D., Huang, Q., Robinson, C. V., Horwitz, J., and Eisenberg, D. (2010) Crystal structures of truncated alphaA and alphaB crystallins reveal structural mechanisms of polydispersity important for eye lens function. *Protein Sci. 19*, 1031−1043.
(29) Flaugh, S. L., Kosinski-Collins, M. S., and King, J. (2005) Contributions of hydrophobic domain interface interactions to the folding and stability of human gammaD-crystallin. *Protein Sci. 14*, 569−581.
(30) Papanikolopoulou, K., Mills-Henry, I., Thol, S., Wang, Y., Gross, A., Kirschner, D., Decatur, S., and King, J. (2008) Formation of amyloid fibrils in vitro by human γD-crystallin and its isolated domains. *Mol. Vision 14*, 81−89.
(31) Wang, Y., Petty, S., Trojanowski, A., Knee, K., Goulet, D., Mukerji, I., and King, J. (2010) Formation of amyloid fibrils in vitro from partially unfolded intermediates of human γC-crystallin. *Invest. Ophthalmol. Visual Sci. 51*, 672−678.
(32) Moran, S. D., Woys, A. M., Buchanan, L. E., Bixby, E., Decatur, S. M., and Zanni, M. T. (2012) Two-dimensional IR spectroscopy and segmental ^{13}C labeling reveals the domain structure of human γD-crystallin amyloid fibrils. *Proc. Natl. Acad. Sci. U.S.A. 109*, 3329−3334.
(33) Fink, A. L. (1998) Protein aggregation: folding aggregates, inclusion bodies and amyloid. *Folding Des. 3*, R9−R23.
(34) Hemmingsen, J. M., Gernert, K. M., Richardson, J. S., and Richardson, D. C. (1994) The tyrosine corner: A feature of most Greek key beta-barrel proteins. *Protein Sci. 3*, 1927−1937.
(35) Burley, S. K., and Petsko, G. A. (1985) Aromatic-aromatic interaction: a mechanism of protein structure stabilization. *Science 229*, 23−28.
(36) Xia, Z., Yang, Z., Huynh, T., King, J. A., and Zhou, R. (2013) UV-radiation induced disruption of dry-cavities in human γD-crystallin results in decreased stability and faster unfolding. *Sci. Rep. 3*, 1560.

(37) Borkman, R., and Phillips, S. (1985) Tyrosine-to-tryptophan energy transfer and the structure of calf gamma-II crystallin. *Exp. Eye Res. 40*, 819−826.
(38) Moens, P. D. J., Helms, M. K., and Jameson, D. M. (2004) Detection of tryptophan to tryptophan energy transfer in proteins. *Protein J. 23*, 79−83.
(39) Li, D., Borkman, R., Wang, R., and Dillon, J. (1990) Mechanisms of photochemically produced turbidity in lens protein solutions. *Exp. Eye Res. 51*, 663−669.
(40) Borkman, R. F., Tassin, J. D., and Lerman, S. (1981) The rates of photodestruction of tryptophan residues in human and bovine ocular lens proteins. *Exp. Eye Res. 32*, 747−754.
(41) Andley, U. P., and Clark, B. A. (1989) The effects of near-UV radiation on human lens beta-crystallins: Protein structural changes and the production of O_2^- and H_2O_2. *Photochem. Photobiol. 50*, 97−105.
(42) Finley, E. L., Busman, M., Dillon, J., Crouch, R. K., and Schey, K. L. (1997) Identification of photooxidation sites in bovine alpha-crystallin. *Photochem. Photobiol. 66*, 635−641.
(43) Simpanya, M. F., Ansari, R. R., Leverenz, V., and Giblin, F. J. (2008) Measurement of lens protein aggregation in vivo using dynamic light scattering in a guinea pig/UVA model for nuclear cataract. *Photochem. Photobiol. 84*, 1589−1595.
(44) Zigman, S., Paxhia, T., McDaniel, T., Lou, M. F., and Yu, N. T. (1991) Effect of chronic near-ultraviolet radiation on the gray squirrel lens in vivo. *Invest. Ophthalmol. Visual Sci. 32*, 1723−1732.
(45) Giblin, F. J., Lin, L.-R., Leverenz, V. R., and Dang, L. (2011) A class I (Senofilcon A) soft contact lens prevents UVB-induced ocular effects, including cataract, in the rabbit in vivo. *Invest. Ophthalmol. Visual Sci. 52*, 3667−3675.
(46) Hibbard, L. B., Kirk, N. J., and Borkman, R. F. (1985) The in vitro photolysis of whole rat lenses using focused 290 nm laser radiation. *Exp. Eye Res. 40*, 285−295.
(47) Mills, I., Flaugh, S., Kosinski-Collins, M., and King, J. (2007) Folding and stability of the isolated Greek key domains of the long-lived human lens proteins γD-crystallin and γS-crystallin. *Protein Sci. 16*, 2427−2444.
(48) Kosinski-Collins, M., and King, J. (2003) In vitro unfolding, refolding, and polymerization of human γD crystallin, a protein involved in cataract formation. *Protein Sci. 12*, 480−490.
(49) Kosinski-Collins, M. S., Flaugh, S. L., and King, J. (2004) Probing folding and fluorescence quenching in human gammaD crystallin Greek key domains using triple tryptophan mutant proteins. *Protein Sci. 13*, 2223−2235.
(50) Moreau, K. L., and King, J. (2009) Hydrophobic core mutations associated with cataract development in mice destabilize human γD-crystallin. *J. Biol. Chem. 284*, 33285−33295.
(51) Kong, F., and King, J. (2011) Contributions of aromatic pairs to the folding and stability of long-lived human γD-crystallin. *Protein Sci. 20*, 513−528.
(52) Chen, J., Flaugh, S. L., Callis, P. R., and King, J. (2006) Mechanism of the highly efficient quenching of tryptophan fluorescence in human gammaD-crystallin. *Biochemistry 45*, 11552−11563.
(53) Chen, J., Callis, P. R., and King, J. (2009) Mechanism of the very efficient quenching of tryptophan fluorescence in human gamma D- and gamma S-crystallins: The gamma-crystallin fold may have evolved to protect tryptophan residues from ultraviolet photodamage. *Biochemistry 48*, 3708−3716.
(54) Schafheimer, N., and King, J. (2013) Tryptophan cluster protects human γD-crystallin from ultraviolet radiation-induced photoaggregation in vitro. *Photochem. Photobiol. 89*, 1106−1115.
(55) Moran, S. D., Zhang, T. O., Decatur, S. M., and Zanni, M. T. (2013) Amyloid fiber formation in human γD-crystallin induced by UV-B photodamage. *Biochemistry 52*, 6169−6181.
(56) Yang, Z., Xia, Z., Huynh, T., King, J. A., and Zhou, R. (2014) Dissecting the contributions of β-hairpin tyrosine pairs to the folding and stability of long-lived human γD-crystallins. *Nanoscale* [Online early access], DOI: 10.1039/c1033nr03782g, Published Online: Nov 12, 2013.
(57) MacLean, B., Tomazela, D. M., Shulman, N., Chambers, M., Finney, G. L., Frewen, B., Kern, R., Tabb, D. L., Liebler, D. C., and MacCoss, M. J. (2010) Skyline: An open source document editor for creating and analyzing targeted proteomics experiments. *Bioinformatics 26*, 966−968.
(58) Lakowicz, J. R. (1999) Energy transfer, In *Principles of Fluorescence Spectroscopy*, 2nd ed., pp 368−391, Kluwer Academic/Plenum Publishers, New York.
(59) Kettenhofen, N. J., and Wood, M. J. (2010) Formation, reactivity, and detection of protein sulfenic acids. *Chem. Res. Toxicol. 23*, 1633−1646.
(60) McCall, J. D., and Anseth, K. S. (2012) Thiol−ene photopolymerizations provide a facile method to encapsulate proteins and maintain their bioactivity. *Biomacromolecules 13*, 2410−2417.
(61) Reddie, K. G., and Carroll, K. S. (2008) Expanding the functional diversity of proteins through cysteine oxidation. *Curr. Opin. Chem. Biol. 12*, 746−754.
(62) Fu, X., Mueller, D. M., and Heinecke, J. W. (2002) Generation of intramolecular and intermolecular sulfenamides, sulfinamides, and sulfonamides by hypochlorous acid: A potential pathway for oxidative cross-linking of low-density lipoprotein by myeloperoxidase. *Biochemistry 41*, 1293−1301.
(63) Shen, H., Spikes, J., Kopeeková, P., and Kopeek, J. (1996) Photodynamic crosslinking of proteins. I. Model studies using histidine-and lysine-containing N-(2-hydroxypropyl) methacrylamide copolymers. *J. Photochem. Photobiol., B 34*, 203−210.
(64) Moran, S. D., Decatur, S. M., and Zanni, M. T. (2012) Structural and sequence analysis of the human γD-crystallin amyloid fibril core using 2D IR spectroscopy, segmental ^{13}C labeling, and mass spectrometry. *J. Am. Chem. Soc. 134*, 18410−18416.
(65) Chen, J., Toptygin, D., Brand, L., and King, J. (2008) Mechanism of the efficient tryptophan fluorescence quenching in human γD-crystallin studied by time-resolved fluorescence. *Biochemistry 47*, 10705−10721.
(66) Bova, L. M., Wood, A. M., Jamie, J. F., and Truscott, R. J. (1999) UV filter compounds in human lenses: the origin of 4-(2-amino-3-hydroxyphenyl)-4-oxobutanoic acid O-beta-D-glucoside. *Invest. Ophthalmol. Visual Sci. 40*, 3237−3244.
(67) Streete, I. M., Jamie, J. F., and Truscott, R. J. W. (2004) Lenticular levels of amino acids and free UV filters differ significantly between normals and cataract patients. *Invest. Ophthalmol. Visual Sci. 45*, 4091−4098.
(68) Xing, K., and Lou, M. (2010) Effect of age on the thioltransferase (glutaredoxin) and thioredoxin systems in the human lens. *Invest. Ophthalmol. Visual Sci. 51*, 6598−6604.
(69) Siegfried, C. J., Shui, Y.-B., Holekamp, N. M., Bai, F., and Beebe, D. C. (2010) Oxygen distribution in the human eye: Relevance to the etiology of open angle glaucoma after vitrectomy. *Invest. Ophthalmol. Visual Sci. 51*, 5731−5738.
(70) Andley, U. P., Malone, J. P., and Townsend, R. R. (2011) Inhibition of lens photodamage by UV-absorbing contact lenses. *Invest. Ophthalmol. Visual Sci. 52*, 8330−8341.
(71) Giblin, F. J., Lin, L.-R., Simpanya, M. F., Leverenz, V. R., and Fick, C. E. (2012) A class I UV-blocking (senofilcon A) soft contact lens prevents UVA-induced yellow fluorescence and NADH loss in the rabbit lens nucleus in vivo. *Exp. Eye Res. 102*, 17−27.
(72) Babizhayev, M. A., Burke, L., Micans, P., and Richer, S. P. (2009) N-Acetylcarnosine sustained drug delivery eye drops to control the signs of ageless vision: Glare sensitivity, cataract amelioration and quality of vision currently available treatment for the challenging 50,000-patient population. *Clin. Interventions Aging 4*, 31−50.
(73) Ha, J.-w., Schwahn, A. B., and Downard, K. M. (2010) Ability of N-acetylcarnosine to protect lens crystallins from oxidation and oxidative damage by radical probe mass spectrometry (RP-MS). *Rapid Commun. Mass Spectrom. 24*, 2900−2908.

(74) Shi, Q., Yan, H., Li, M.-Y., and Harding, J. J. (2009) Effect of a combination of carnosine and aspirin eye drops on streptozotocin − induced diabetic cataract in rats. *Mol. Vision 15*, 2129−2138.
(75) Nahomi, R. B., Wang, B., Raghavan, C. T., Voss, O., Doseff, A., Santhoshkumar, P., and Nagaraj, R. H. (2013) Chaperone peptides of α-crystallin inhibit epithelial cell apoptosis, protein insolubilization and opacification in experimental cataracts. *J. Biol. Chem. 288*, 13022−13035.
(76) Ray, M. E., Wistow, G., Su, Y. A., Meltzer, P. S., and Trent, J. M. (1997) AIM1, a novel non-lens member of the betagamma-crystallin superfamily, is associated with the control of tumorigenicity in human malignant melanoma. *Proc. Natl. Acad. Sci. U.S.A. 94*, 3229−3234.